



Journal of Applied Sciences

ISSN 1812-5654

science
alert

ANSI*net*
an open access publisher
<http://ansinet.com>

New Way to Find the Modulus of Elasticity

Arshed Abdulhamed Mohammed, Sallehuddin Mohamed Haris and Mohd Zaki Nuawi
Department of Mechanical and Materials Engineering, Faculty of Engineering and the Built Environment,
University Kebangsaan Malaysia, 43600, UKM Bangi, Selangor, Malaysia

Abstract: There are a real and irregular difference between the modulus of elasticity calculated from traditional tensile test and the modulus of elasticity calculated by evaluating time of wave flying. This study provides a new method of calculating the modulus of elasticity with high accuracy, for a broad spectrum of solid materials, using ultrasonic piezoelectric transducers. Two stages are included in this method; each using a pitch-catch method to determine the difference in wave amplitude between the actuator and the sensor. In order to achieve this, the ultrasonic transfer functions of the actuator and the sensor using Masons equivalent circuit (transmission line), were derived. In addition, many variables were detected in this calculation, such as the attenuation and reflection of the wave passing through the test pieces. A new relationship between the output voltage and the modulus of elasticity was derived. Each of the steps, such as obtaining the responses of the function generator and the transfer functions, were compared many previous studies within this field and the results were very close. Finally, the accuracy of this new method reached 99-98% when comparing real magnitudes of modulus of elasticity, from approximately 40 types of materials, tested to ensure the validity of the results.

Key words: Static modulus of elasticity, dynamic, piezoelectric, electrodes, actuator, sensor, transducer

INTRODUCTION

A modulus of elasticity is one of important materials properties. It was regarded a measurement of material rigidity, endurance limit, longitudinal velocity and many other properties. Although, the study of this variable had started long ago (Forster and Koster, 1939) the relation between the modulus of elasticity of many materials and its damping ratio were studied but so far, continued to evolve with the development of new materials and techniques.

Since, Eurocode1 (2003) recommended depending two values of modulus of elasticity. First, static modulus of elasticity (E_s) (loaded modulus of elasticity) that can get it from loading test like traditional tensile tests and another type is a dynamic modulus of elasticity (E_D) (unloaded) that can be get it from unloading tests like acoustic tests (Stasiak *et al.*, 2007), especially that uses piezoelectric transducer and which was chosen in this study as a method to calculate the modulus of elasticity.

There are wildly using ultrasonic relationships for testing the materials properties like:

$$E = 2\rho C_s^2 (1+\nu)$$

where, E is in MPa, ρ is in kg m^{-3} , C_s is the acoustic shear waves speed (m sec^{-1}) and ν is the poisson's ratio.

To calculate the modulus of elasticity, Ciccotti and Mulargia (2004) used this equation to calculate the dynamic modulus of elasticity and compared it with static modulus of elasticity for seismogenic rock (in Italian Apennines) and found the dynamic modulus was greater (10%) than static modulus. Also by using pulse-echo technique, OLYMPUS (2011) referred to use this relationship to calculate the modulus of elasticity for different materials but the problem of this method was the increasing of difference between the static and dynamic modulus of elasticity with increasing of the density of specimen (Builes *et al.*, 2008). This study proposed a new acoustic method to calculate the static modulus of elasticity with high accuracy and for wide range of solid materials.

In another hand, many studies were published in this field but did not refer to this different between E_D and E_s . Far from traditional methods, there are several tests done to measure it where, Fang *et al.* (1995) measured modulus of elasticity of an adsorbed monolayer by developing diffusion penetration theory. Garnier and Corneloup (1996) used the analysis of surface wave propagation in material to calculate the modulus of elasticity for many nitride layers. Also just for special materials (not as general method) (Bray *et al.*, 1997; Bastida *et al.*, 1998; Chow and Millos, 1999; Gorninski *et al.*, 2004; Chen *et al.*, 2009; Vendra and Rabiei, 2010;

Corresponding Author: Arshed Abdulhamed Mohammed, Department of Mechanical and Materials Engineering,
Faculty of Engineering and the Built Environment, University Kebangsaan Malaysia, 43600, UKM Bangi,
Selangor, Malaysia Tel: +60108916964

Osamura *et al.*, 2010; Diaz *et al.*, 2011), measurement the modulus of elasticity (by employing experimental work) for Nb and Sn, polymers (Epoxy Impregnated Niobium-Tin and Niobium-Titanium Composites) (polymer concrete and Portland cement concrete), NiTi shape memory alloy, composite metal foams, BSCCO tapes and (plastics and wood plastic composites), respectively. So several researches used mathematical methods to investigate or detect it. Gokceoglu and Zorlu (2004) chose a Fuzzy logic as a method to calculate the modulus of elasticity of problematic rock. Dehghan *et al.* (2010) managed to find a general mathematical method to estimate it for many materials when they used regression and artificial neural networks.

A piezoelectric transducer is widely used in these types of tests not for materials test but also in another science tests. Greve *et al.* (2008) succeeded to replace a disturbance force effects on steel squire plate 19×19×305 mm length, width and thickness, respectively by piezoelectric transducer with center frequency 2.2 MHz and glue it by Cyanoacrylate adhesive to create longitudinal sound wave but they use complex electric source to drive this transducer (five-cycle windowed sinusoid voltage waveform). This study is close to some of these assumptions because it used pitch catch technique but the type piezoelectric transducer which was chosen here with two aluminum electrodes. Also for the same reasons, Piazza *et al.* (2004) and Chao *et al.* (2001) used these types of electrodes. Lee and Huang (2002) studied the mechanical effects of aluminum, silver and gold electrodes on the vibrations of quartz crystal plates for piezoelectric transducer.

Joseph and Charles (1996) illustrated many relations for several parameters in this field (Fig. 1). The modulus of elasticity can be detected as shown in Eq. 1:

$$\frac{1}{\Gamma} = \left(\frac{1}{4}\right) \left(\sqrt{\frac{E_1 \rho_1}{E_2 \rho_2}} + \sqrt{\frac{E_2 \rho_2}{E_1 \rho_1}} \right)^2 \quad (1)$$

where, Γ is the longitudinal vibration transmission efficiency:

$$r = \begin{cases} h_2/h_1 & \text{for plat (h plat thickness)} \\ A_2/A_1 & \text{for beam (across section area of beam or plate)} \end{cases}$$

E is modulus of elasticity, ρ is density, f is frequency (Hz), l structural components on which waves approach and leave discontinuity response and m is total mass.

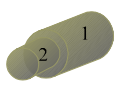
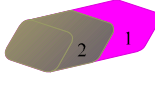
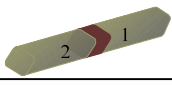
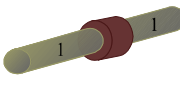
Shape	The longitudinal vibration transmission efficiency
	$\frac{1}{\Gamma} = \frac{1}{4} \left(\sqrt{r} + \sqrt{\frac{1}{r}} \right)^2$
	$\frac{1}{\Gamma} = \left(\frac{1}{4}\right) \left(\sqrt{\frac{E_1 \rho_1}{E_2 \rho_2}} + \sqrt{\frac{E_2 \rho_2}{E_1 \rho_1}} \right)^2 \quad (1)$
	$\frac{1}{\Gamma} = \left(\frac{f}{f_1}\right)^2$
	$\frac{1}{\Gamma} = 1 + \left(\frac{f}{f_m}\right)^2$

Fig. 1: A vibration transmission of structural discontinuities

THEORY AND METHODOLOGY

The idea of this study depends on choosing aluminum as material for test other materials. The value of product the density (ρ_1) with modulus of elasticity (E_1) for aluminum is regarded one of lowest values comparing with the other materials. Therefore, the relationship between the transmission efficiency produced from change the materials (from aluminum to another materials) and ($\rho \times E$) for other materials was smooth and quite.

The concept of designing an instrument to calculate the modulus of elasticity for a specimen will involve two steps following the same processes:

Step 1: This step involves putting the aluminum specimen in between two elements of Piezoelectric Ceramic Transducer (PCT) where the first element acts as an actuator and the other as the receiver as shown in Fig. 2a, b. The actuator will be connected to a pulse generator. The receiver will be connected to an amplifier then to an oscilloscope. When the pulse of voltage (which produced from pulse generator) is applied on the actuator directly, the actuator will change the input pulse of voltage to vibration wave which will pass through the aluminum and then it will reach the receiver which has the ability to convert the vibration wave to an electrical signal. The reduction in the amplitude of voltage wave (which will be read in the oscilloscope) will be

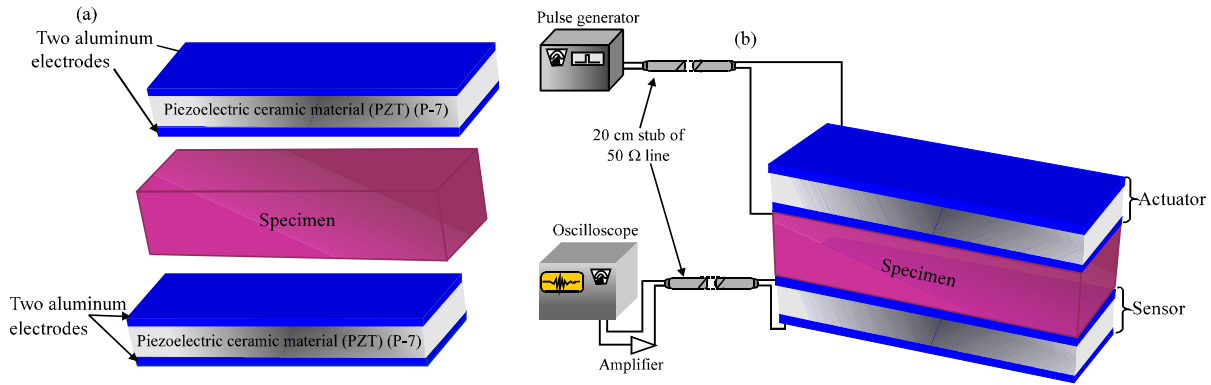


Fig. 2(a-b): (a) Specimen with two elements of piezoelectric where each element with two electrodes and (b) Location of specimen between the two elements of piezoelectric

proportional to the reduction in the transient vibration wave amplitude that will pass through the aluminum piece. The purpose of this step is calculation of the transmission efficiency, where the vibration wave will suffer a reduction in amplitude for many reasons such as attenuation or reflection from boundaries (surfaces) of the aluminum piece, etc

Step 2: The same procedure will be followed for the other specimens but for a different purpose. This purpose is to calculate transmission efficiency that is produced from changing the materials in addition to another previous reasons as shown in Fig. 2b

PCT (actuator and sensor): PCT is widely use in the ultrasonic testing of materials. The dimensions and the type of material of piezoelectric transducer determine the response of it, depending on this and according to instructors for one of PCTs manufacturing companies (MURATA company) (MURATA, 2005), thick mode transducer made of Lead Zirconate Titanate (PZT) P-7 was chosen for dual use, for the actuator and the sensor, where this material has large electromechanical coupling coefficient (ϕ) and large value of piezoelectric constant (d).

Mason transmission line technique was chosen as a method for getting the equivalent circuit, then by using Laplace transformer, the transfer functions for these transducers were driven. This circuit represents the conversion of electric energy to mechanical energy and vice versa as shown in Fig. 3. A transmission line technique was chosen as analysis method because it does not depend only on the output response of PCT to building the transfer function like using fuzzy logic (Sofla *et al.*, 2010) and genetic algorithm (Fabijanski and Lagoda, 2008, 2010) but it also takes

in its accounting the effect of most parameter of piezoelectric material as shown with details in Fig. 3. Mohammed *et al.* (2014) proposed a new and high accuracy mathematical model for PCT, this PCT has two silver electrodes. Therefore, this study chose this mathematical model to analyze the performance of PCT but the different here is the type of electrodes (aluminum instead of silver).

V and I are voltage and current at the electric terminal. U_1 , F_1 and U_2 , F_2 represent front and back-face velocities and radiation forces of piezoelectric plate, respectively. According to choosing P-7 as material for PCT and to getting a small size of this transducer, the dimensions of PCT and other parameters were listed in Table 1.

W_1 and W_2 (Fig. 3) represent the facing and backing load resistance, here in this study the two aluminum electrodes represented these loads in both said of piezoelectric plate. The characteristic impedance of any medium contain real and imaginary parts but for solid and liquid materials, the imaginary is very small comparing to real part, therefore the impedance of solid and liquid materials can be consider as a real. As a result of this, $W_1 = W_2 = W = \rho Au = 6855.4 \Omega$, where for aluminum $\rho = 2699 \text{ kg m}^{-3}$, $A = 4 \times 10^{-4} \text{ m}$ and $u = 6350 \text{ m sec}^{-1}$.

$$F_1 = -U_1 R_1 \quad (2)$$

$$F_2 = -U_2 R_2 \quad (3)$$

After taking laplace transform for parameters Z_1 and Z_2 in Mason equivalent circuit (Fig. 3), the following equations are obtained:

$$Z_1 = \frac{2Z_0}{e^{sT} - e^{-sT}} \quad (4)$$

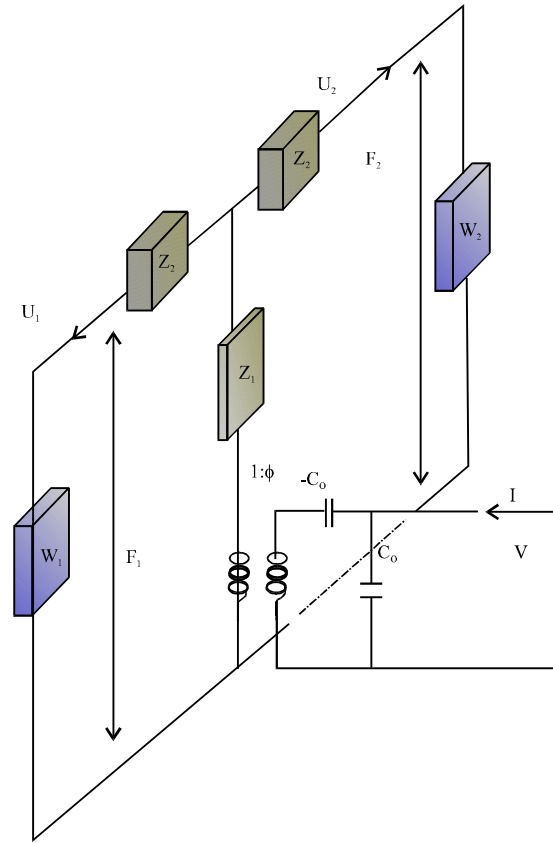


Fig. 3: Mason equivalent-circuit of thick mode piezoelectric plat transducer

Table 1: Details of elements and parameters of equivalent circuit of piezoelectric plate

Parameters	Magnitude	Physical relationship
(t) thickness of piezoelectric (m)	3.02×10^{-3}	From material properties
(A) effective area of piezoelectric, respectively (m ²)	4×10^{-4}	
(Y ₃₃) elastic constant (N m ⁻²)	5.5×10^{10}	
(ρ) density (kg m ⁻³)	7.8×10^3	
(d ₃₃) piezoelectric constant (m/v)	410×10^{-12}	
(ε ₃₃) dielectric constant (farad/m)	1.8585×10^{-8}	
(Z ₁) and (Z ₂) impedance represent the ceramic as lossless mechanical transmission line of length l		$Z_1 = jZ_0 \tan\left(\frac{\omega l}{2v}\right)$ $Z_2 = \frac{-jZ_0}{\sin\left(\frac{\omega l}{v}\right)}$
(u) propagation velocity along the thickness (m/s)	2655.4	$\mu = \sqrt{\frac{Y_{33}}{\rho}}$
(Ω) resonance frequency KHz (1/sec)	885.14	$\omega = \mu/2t$
(h ₃₃) piezoelectric constant (electric field /strain under constant charge) (v/m)	2.439×10^9	$h_{33} = 1/d_{33}$
(C ₀) static capacitance (Farad)	4.95×10^{-9}	$C_0 = A \times \frac{\epsilon_{33}^T}{t}$
(Z ₀) characteristic acoustic impedance of the plate (Ω)	8284.8	$Z_0 = \rho Au$
(φ) transformer voltage ratio (N/v)	12.09	$\phi = C_0 h_3$
(T) time delay for acoustic wave to travel from one electrode to another (sec)	5.64888×10^{-7}	$T = t/u$

$$Z_2 = \frac{Z_0(1 - e^{-sT})}{1 + e^{-sT}} \quad (5)$$

$$2Z_1 + Z_2 = Z_0 \frac{(1 + e^{-sT})}{1 - e^{-sT}} \quad (6)$$

By employing conventional analysis, the relation between variables at the three ports in Fig. 3 can be expressed as a matrix as below (Challis and Harrison, 1983; Alwi *et al.*, 1996, 2000):

$$\begin{bmatrix} F_1 \\ F_2 \\ V \end{bmatrix} = \begin{bmatrix} Z_1 + Z_2 & Z_1 & \frac{\phi}{sC_o} \\ Z_1 & Z_1 + Z_2 & \frac{\phi}{sC_o} \\ \frac{\phi}{sC_o} & \frac{\phi}{sC_o} & \frac{1}{sC_o} \end{bmatrix} \begin{bmatrix} U_1 \\ U_2 \\ I \end{bmatrix} \quad (7)$$

Commonly, the actuator is connected to voltage source pulse generator but in order to getting maximum transmitted power, the impedance of transducer must be close to 50 Ω. Therefore, two lines of a 20 cm stub of 50 Ω ($R_n = 50 \Omega$) were used, first line was connected between pulse generator and the actuator and the other between the sensor and the oscilloscope as shown in Fig. 2b. This stub line already was on parallel with transducer circuit to be with the impedance of transducer close to impedance of pulse generator as shown in Fig. 4. As well as for the oscilloscope in another side.

Because of the symmetric shape, components and load ($W_1 = W_2 = W$) in both said of Mason transmission line circuit as shown in Fig. 3, therefore, $F_1 = F_2$, also, $U_1 = U_2 = U$, so by using the first or second relationship in Eq. 3, we can get:

$$-WU = (Z_1 + Z_2)U + Z_1U + \frac{\phi I}{sC_o} \quad (8)$$

$$U = -\frac{\phi I}{(W + 2Z_1 + Z_2)sC_o} \quad (9)$$

also from third relation in Eq. 7:

$$V = \frac{2\phi U}{sC_o} + \frac{I}{sC_o} \quad (10)$$

and:

$$Z_T = \frac{V}{I} = \frac{-2\phi^2 + (W + 2Z_1 + Z_2)sC_o}{(sC_o)^2(W + 2Z_1 + Z_2)} \quad (11)$$

According to Fig. 4b, we get:

$$Z_T = \frac{VR}{V_r - V} \quad (12)$$

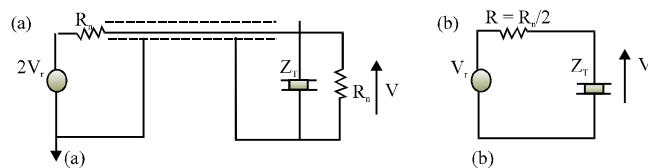


Fig. 4(a-b): (a) Specimen with circuit connection of piezoelectric impedance (Z_T) and pulse generator $2V_r$ by a matched line of characteristic impedance R_n and (b) Equivalent Thevenin circuit for Fig. 4a

By equating Eq. 11 = 12:

$$\frac{V}{V_r} = \frac{sC_o W + (2Z_1 + Z_2)sC_o - 2\phi^2}{(sC_o)^2 R W + sC_o W + R(sC_o)^2 (2Z_1 + Z_2)sC_o (2Z_1 + Z_2) - 2\phi^2} \quad (13)$$

By putting Eq. 6 in Eq. 13:

$$= \frac{sC_o W + (1 - e^{-sT}) + Z_o sC_o (1 + e^{-sT}) - 2\phi^2 (1 - e^{-sT})}{sC_o W (sC_o R + 1)(1 - e^{-sT}) + sC_o Z_o (sC_o R + 1)(1 + e^{-sT}) - 2\phi^2 (1 - e^{-sT})} \quad (14)$$

After inverting e^{-sT} to $1/e^{sT}$ then in simplified Eq. 14 and by using Taylor series we get:

$$e^{sT} = 1 + \frac{sT}{1!} + \frac{(sT)^2}{2!} + \frac{(sT)^3}{3!} + \frac{(sT)^4}{4!} \quad (15)$$

where, V is the value of voltage at both ends of transducer in Fig. 4b. Actually, here V is the electric concept for the output of this circuit, while in our case, this transducer works as actuator therefore, the output of this transducer is vibration wave, where $V = F/\phi$ and by taking Laplace $\mathcal{L}(F/\phi) = (F)_{(s)}/\phi$. $V_r = 10$ volt as pulse, $\mathcal{L}(V_r) = P \times (V_r)_{(s)}$, where, $P = 10$ and substituting from Eq. 15 in 14, then simplified the produced equation and replacing V by F/ϕ , we get:

$$\frac{F_{(s)}}{V_{r(s)}} = \frac{A_4 s^4 + A_3 s^3 + A_2 s^2 + A_1 s + A_0}{B_5 s^5 + B_4 s^4 + B_3 s^3 + B_2 s^2 + B_1 s + B_0} \quad (16)$$

Where:

$$A_0 = (D - L - 2T\phi^2) = -7.5324 \times 10^{-4}$$

$$A_1 = \left(TD - \frac{2T^2\phi^2}{2!} \right) \phi = -1.5247 \times 10^{-10}$$

$$A_2 = \left(\frac{DT^2}{2!} - \frac{2T^3\phi^2}{3!} \right) \phi = 5.2251 \times 10^{-17}$$

$$A_3 = \left(\frac{DT^3}{3!} - \frac{2T^4\phi^2}{4!} \right) \phi = 4.0053 \times 10^{-23}$$

$$A_4 = \left(\frac{DT^4}{4!}\right)\phi = \left(\frac{(K+H)T^4}{4!}\right)\phi = 2.7311 \times 10^{-29}$$

$$\frac{\lambda_1}{\lambda_2} = \frac{c_1}{c_2} \rightarrow f_1 = f_2$$

$$B_0 = D - L - 2T\phi^2 = (2K - 2\phi^2 T) = -8.369 \times 10^{-5}$$

$$B_1 = DN - LN + TD - \frac{2T^2\phi^2}{2!} = -1.6942 \times 10^{-11}$$

$$B_2 = DNT + \frac{DT^2}{2!} - \frac{2T^3\phi^2}{3!} = 1.207 \times 10^{-17}$$

$$B_3 = \frac{DNT^2}{2!} + \frac{DT^3}{3!} - \frac{2T^4\phi^2}{4!} = 3.1875 \times 10^{-25}$$

$$B_4 = \frac{DNT^3}{3!} + \frac{DT^4}{4!} = 4.1287 \times 10^{-30}$$

$$B_5 = \frac{DNT^4}{4!} = 2.7994 \times 10^{-37}$$

After the Transfer Functions (TF) of the actuator, the same technique was used to find TF of sensor, all the system can be represented by using Simulink MATLAB.

The two transfer functions were tested by connection of a pulse generator with first TF which belong to the actuator then the gain (this gain represented the losing in intensity of the wave, then with second TF which belong to sensor, next with amplifier, finally with oscilloscope as shown in Fig. 5. This system was tested by using Simulink MATLAB to make sure from these functions.

First let, C(t) represented the response of the actuator before entering the specimen, W(t) was the vibration wave got out from the specimen (before entering the sensor) and Y(t) was the response of sensor. The response of the actuator and sensor according to the Eq. 15 were explained in Fig. 6a and b, while Fig. 6c and d represented the greatest wave of the front face of PCT for the actuator and sensor, respectively.

Attenuation and reflection of vibration wave through aluminum specimen: The wave generated from actuator direct delivers from the aluminum electrodes to the specimen as shown in Fig. 2. Depending on Snell's law, the frequency stays constant during passing the wave through different materials in spite of different in densities:

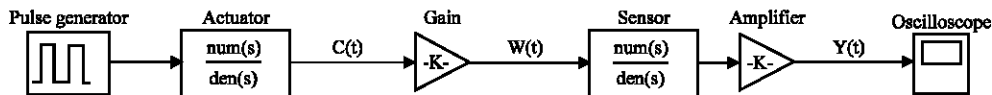


Fig. 5: Schematic showing all system by using Simulink MATLAB

where, $f = c/\lambda$ and λ is the wave length).

The designing of this test was avoided many assumptions that effect on the wave propagation (no cross-section change, no resilient insert and no blocking mass) as explained in Fig. 1 except the change in materials. According to the waves attenuation relationship $P = P_0 e^{-\alpha x}$ where, P_0, P are sound pressure at the start point and at the end respectively, α was the attenuation coefficient and x was the section length, so the attenuation diagram (attenuation diagram page 577 in the appendix of (Krautkramer and Krautkramer, 1990) illustrated in the right side of it the relationship between the thickness of material and the magnitudes of attenuation in dB for widely range of materials. Here, all section length (thickness of the specimen) within the limit 1-5 mm to avoid the high effective of attenuation where the magnitude of attenuation for most solid materials at this range of thickness is around 1.8%. Also, the other dimensions of the specimen was a rectangular dimensions, where the length×width = 25×25 mm. The effective reflecting waves from surfaces of specimen was very small, that may cause a little noise and it can cancel it from calculations where all section length within near field of piezoelectric actuator (Olympus, 2006). According to the specific properties of the chosen equipments, the limitation of this method was the thickness of specimen, where the thickness must not exceed the 1-5 mm.

CALCULATION OF THE TOTAL TRANSMISSION EFFICIENCY (Γ_{TOTAL})

The definition of Γ_{Total} for step 1 or for specimen in step 2, is the percentage of maximum amplitude of existing vibration wave (K_w) from specimen to maximum amplitude of entering vibration wave (K_e) to it ($\Gamma_{Total} = K_w/K_e$) as shown in Fig. 5. Many probability magnitudes of (Γ_{total}) were taken to derive an equation between Γ_{Total} and the output voltage from the sensor as below:

- If $\Gamma_{total} = 100\%$ (Eq. 1)

This case means no loss through passing the vibration wave in the specimen, also means $C(t) = W(t)$ and the magnitude of gain = one (Fig. 5). After

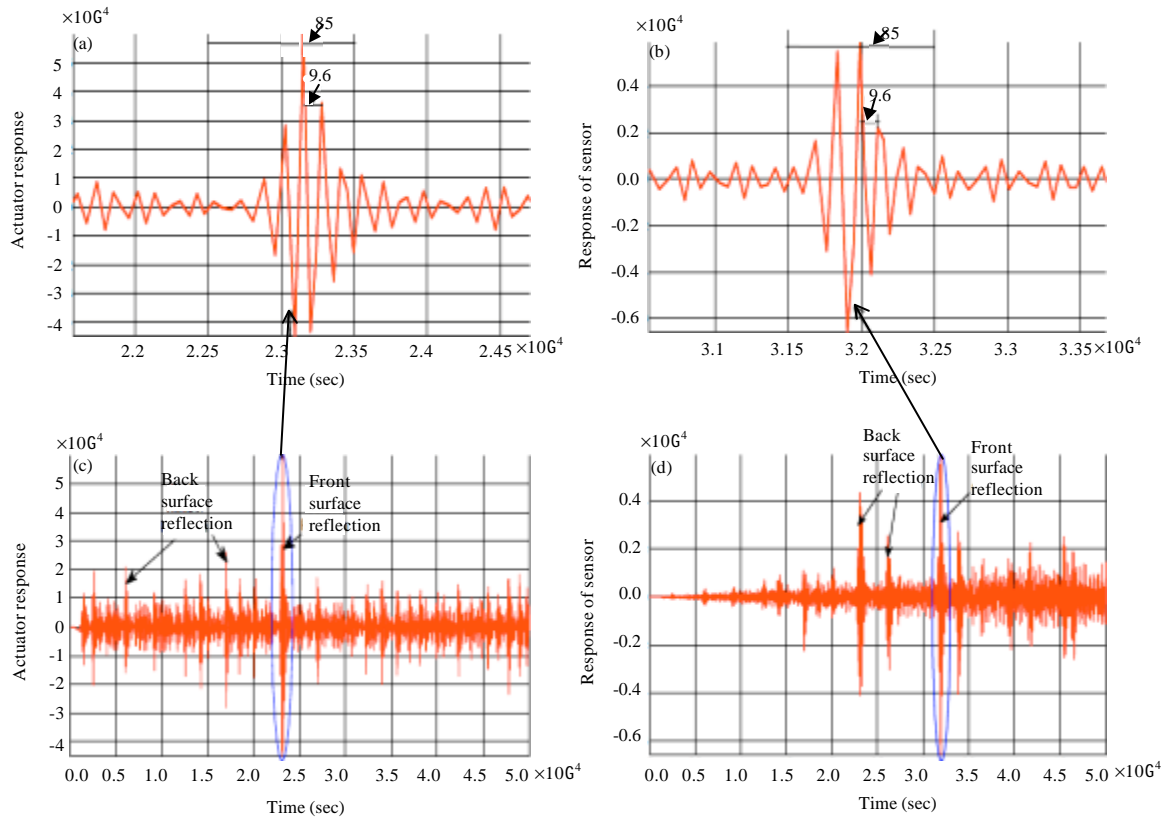


Fig. 6(a-d): Response of the (a) Actuator and (b) Sensor and zoom out of greatest front surface wave reflection for the (c) Actuator and (d) Sensor

Table 2: Changing in magnitudes of Γ_{Total} with $V_s(v)$

(Γ_{total}) (%)	$K_w \times 10^{-4}$	V_s (volt)
100	5.9956	0.58
90	5.3961	0.5219
80	4.7965	0.464
70	4.1968	0.406
60	3.5972	0.348
50	2.9975	0.2899
40	2.398	0.2319
30	1.798	0.174
20	1.1991	0.116
10	0.5996	0.058

using Simulink in MATLAB, the maximum amplitude of the waves were ($K_c = K_w = 5.59956 \times 10^{-4}$ and $V_s = 0.58$ V)

- If $\Gamma_{total} = 90\%$

The same process was repeated but in this case $W(t)$ was less than $C(t)$ with 10% and as a result of this $K_w = 5.3961 \times 10^{-4}$ and $V_s = 0.5219$ V. These processes were repeated also from (80-10%) as shown in Table 2, by using the details in Table 2 and Fig. 7 the Eq. 17 was driven:

$$\Gamma_{total} = 1.724 \times V_s \quad (17)$$

But the total transmission efficiency from Fig. 1 and 2:

$$\Gamma_{total} = [\Gamma_M]^2 \times \Gamma_S \times \Gamma_R \times \Gamma_B \times \Gamma_{O1} \quad (18)$$

Where:

Γ_M = Vibration transmission efficiency producing from changing the material

Γ_S = Vibration transmission efficiency producing from changing the section

Γ_R = Vibration transmission efficiency producing from existing resilient

Γ_B = Vibration transmission efficiency producing from block material

Γ_{O1} = Experimental magnitude of total transmission efficiency that produces from many reasons like the attenuation and the reflection, etc

According to conditions of this test, the value of this efficiency in Eq. 18 was around 98.2%. $\Gamma_R = \Gamma_B = \Gamma_S = 1$ (if there are no resilient, no block material and no cross section change). The $(Z\Gamma_M)^2$ in Eq. 18 produced from $(\Gamma_M \times \Gamma_M)$ where, first term produced from

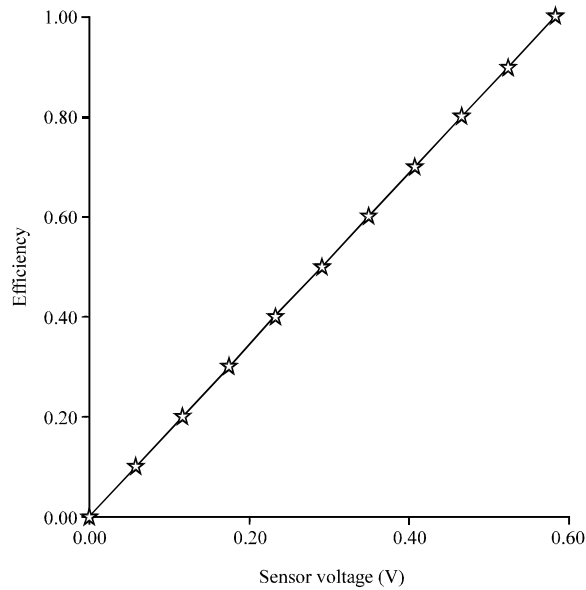


Fig. 7: Relationship between total efficiency (Γ_{Total}) and the output voltage from sensor (V_s)

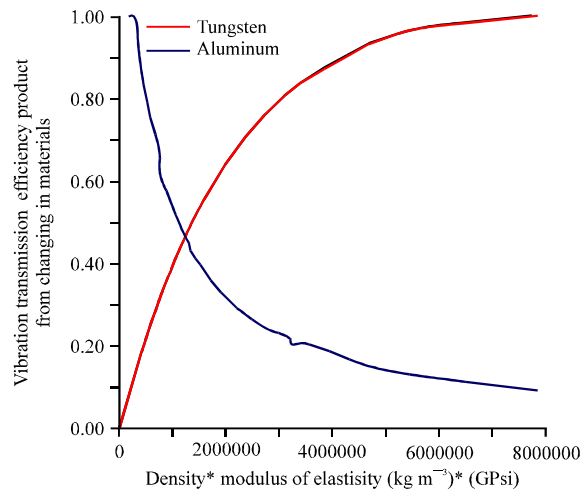


Fig. 8: Relationships between tungsten and aluminum

first changing in materials (from aluminum electrode which belong to actuator to specimen) and the other belong to second changing (from specimen to aluminum electrode which belong to the sensor) as shown in Fig. 2. According to these assumption:

$$\Gamma_M = \sqrt{\Gamma_{Total}/\Gamma_{01}} \tag{19}$$

By using the Eq. 1, Fig. 8 was plotted. Each point in this curve represents the crossing of Γ_M (between aluminum and one of solid materials) from said and $\rho \times E$ for this material from another said, where, ρ is the density and equals 2699 kg m^{-3} and E is the modulus

of elasticity and equals in 70 GPa, where the properties of more than 40 types of the solid materials were chosen to drawn this curve (Cardarelli, 2008). Also, the same processes and calculations were repeated for tungsten instead of aluminum as shown in the Fig. 8.

Two relationships were illustrated in Fig. 8, first the blue curve between Γ_M for the aluminum and the other materials from side and $\rho \cdot E$ for different types of materials from other side. Second (red curve) the same relation but for the tungsten instead of the aluminum.

In addition to previous reasons that were explained about using the aluminum as electrodes, the conductivity

of aluminum electrodes is good and it is not far from level of electric conductivity of silver and gold electrodes.

Actually, the mean reason to choose the aluminum as a constant material to test the other materials is clear in Fig. 8. This was chosen because the aluminum has one of lowest magnitude of modulus of elasticity and density, where, the other materials can make a smooth relationship with it as shown in the Fig. 8. Also, the tungsten can be used instead of the aluminum in this test especially for materials which have a high magnitude of $\rho.E$ because the tungsten also have one of a highest magnitude of $\rho.E$. This process can be done to keeping on the magnitude of transmission wave intensity as shown in Fig. 8 but the mean problem in using the tungsten is the high acoustic impedance of it and that means we need a high power supply. On another side, this method will give a something error if $E_2 \times \rho_2$ of the specimen was less than the aluminum piece ($70 \text{ Gpsi} \times 2699 \text{ kg m}^{-3} = 188930 \text{ Psi. kg m}^{-3}$) because the relationship behavior of Fig. 8, in this case, will change. In another word, for materials that have acoustic impedance much less than aluminum acoustic impedance Z_{AL} ($Z_{AL} = 17.2 \times 10^6 \text{ kg m}^{-2} \text{ sec}^{-1}$) like magnesium ($Z_{mg} = 8 \text{ kg m}^{-2} \text{ sec}^{-1}$), this test will be not successful. Therefore, this case must return the test but by using the tungsten instead of the aluminum to check the results. The tests proved that the other materials cannot be used as a constant material like the aluminum and the tungsten because the other materials will give a curve relationship like hump and this means there are two magnitudes for ($\rho_2 \times E_2$) for the same efficiency Γ_M .

The equivalent polynomial equation for aluminum curve as shown in the Fig. 8 was driven. For getting a high accuracy, the equivalent equations for this curve was divided in three ranges: from $\Gamma_M = (9-76\%)$ as shown in Eq. 20, from $\Gamma_M = (77-96\%)$ as shown in Eq. 21 and from $(97-100\%)$ as shown in Eq. 22 where the accuracy of these three equations respect to Fig. 8 was about (99-98%):

$$E_2 = \left(\frac{1}{D_2}\right) \times 10^{16} \{2.66484 - 39.8466\Gamma_M + 320.458\Gamma_M^2 - 1567.79\Gamma_M^3 + 4910.29\Gamma_M^4 - 10039.3\Gamma_M^5 + 13311.3\Gamma_M^6 - 11013\Gamma_M^7 + 5158.11\Gamma_M^8 - 1042.9\Gamma_M^9\} \quad (20)$$

$$E_2 = \left(\frac{1}{D_2}\right) \times 10^{15} \{5.31443 - 14.2795\Gamma_M + 14.8334\Gamma_M^2 - 5.644\Gamma_M^3\} \quad (21)$$

$$E_2 = \left(\frac{1}{D_2}\right) \times 10^{19} \{1.124768893 - 3.42389\Gamma_M + 3.47435\Gamma_M^2 - 1.17522\Gamma_M^3\} \quad (22)$$

To check the accuracy of these three (Eq. 20-22) another test was done. By using Eq. 1, 20, 21 and 22,

about 40 materials were tested mathematically to evaluate the modulus of elasticity of them, then the results were compared with real values (for modulus of elasticity). The result were very closed especially for tests that used the aluminum electrodes rather than the tests that used tungsten where Fig. 9a, b illustrated some of these results. We can say now, the Eq. 20, 21 and 22 are general equations in this method even if types of PCT change.

Figure 9 illustrated two matters, first the accuracy of this method according to experimental magnitude of modulus of elasticity and comparing between employing the aluminum and tungsten as a constant material in this test.

According to the assumptions, in this study many variables can be added to Eq. 20 and 21 to be more specific: First the Eq. 17 can be added to these equations instead of Γ_M . A good relationship can be got (with accuracy about 96-97%) between output voltage (that appears in oscilloscope) and the modulus of elasticity of the specimen.

After compensation the Eq. 17 in 19 and the value of Γ_{OI} :

$$\Gamma_M = 1.3249908 \times \sqrt{V_s} \quad (23)$$

According to Eq. 17 and 23, the Eq. 24 can be used for the range of voltages from (0.005696-0.329 V):

$$E_2 = \left(\frac{1}{D_2}\right) \times 10^{18} \{2.66484 - 52.796(\sqrt{V_s}) + 562.6(\sqrt{V_s})^2 - 3646.9(\sqrt{V_s})^3 + 15134(\sqrt{V_s})^4 - 40999(\sqrt{V_s})^5 + 72027(\sqrt{V_s})^6 - 78958(\sqrt{V_s})^7 + 49000(\sqrt{V_s})^8 - 13127(\sqrt{V_s})^9\} \quad (24)$$

And Eq. 25 for the range of voltages from 0.3377-0.52495 V:

$$E_2 = \frac{10^{15}}{D_2} \{5.31443 - 18.920206(\sqrt{V_s}) + 26.041526(\sqrt{V_s})^2 - 1312882(\sqrt{V_s})^3\} \quad (25)$$

And Eq. 26 for the range of voltages from 0.53594-0.5696 V:

$$E_2 = \frac{10^{19}}{D_2} \{1.124768893 - 4.53662(\sqrt{V_s}) + 6.09957(\sqrt{V_s})^2 - 6.35907(\sqrt{V_s})^3\} \quad (26)$$

RESULTS

A specimen made of steel was chosen as test spaceman to know the modulus of elasticity (E_2) of it. This specimen was formed as to be larger than PCT area. Evaluation of the density ρ_2 for specimen is $\rho_2 = \text{mass/volume}$ therefore, $\rho_2 = 7800 \text{ kg m}^{-3}$.

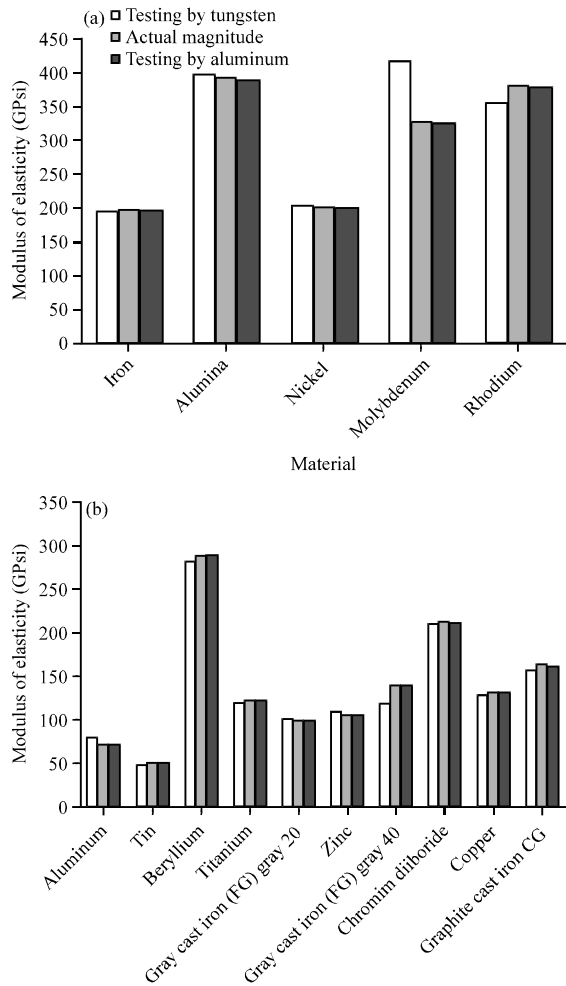


Fig. 9(a-b): Accuracy according to (a) Experimental magnitude of modulus of elasticity and (b) comparison between employing the aluminum and tungsten as a constant material

According to two steps in section 2:

Step 1: Practically, after putting the aluminum piece (Fig. 2) between actuator and sensor, the maximum amplitude in output voltage in oscilloscope was 0.56956 V. For analyzing this result, step 1, must we start from equation of attenuation $P = P_0 e^{-\alpha x}$ where, $P_0 = 5.9956$ dB (from Table 2), $\alpha = 3$ (Krautkramer and Krautkramer, 1990) (roughly for aluminum) and $x = 0.005$ m, this means $p = 5.9063$ dB. So, the percentage between maximum amplitude of output to input for aluminum piece was $5.9063/5.9956 = 98.2\%$, this percentage represents the gain in Fig. 5 and also means $\Gamma_{O1} = 98.2\%$

By using Simulink as shown in Fig. 5, the magnitude of V_s was 0.56956 V, where for pulse generator, the period between two successive pulse was 0.01 sec, pulse width 1×10^{-12} and time of Simulink 0.5×10^{-3} sec. According to Eq. 18 and step 1, step 1 Γ_{O1} equals Γ_{Total} because there are no change material and intersection also no resilient or block material, therefore $\Gamma_M = \Gamma_S = \Gamma_R = \Gamma_B = 1$. Also, $\Gamma_{O1} = 98.2\%$ for other materials because the slim of thickness of specimen make most materials have the same attenuation factor.

Step 2: The practical reading was $V_s = 0.0812$ V, this result appeared on oscilloscope after put the specimen between actuator and receiver. Mathematically, we have two ways, first by using the Eq. 18, where from this equation $\Gamma_M = 37.662\%$, then by using Eq. 20:

$$E_2 = (1/D_2) \times [25814400 - (3.71886 \times 10^8) \Gamma_M + (2.86537 \times 10^9) \Gamma_M^2 - (1.33888 \times 10^{10}) \Gamma_M^3 + (4.00174 \times 10^{10}) \Gamma_M^4 - (7.81666 \times 10^{10}) \Gamma_M^5 + (9.92622 \times 10^{10}) \Gamma_M^6 - (7.89037 \times 10^{10}) \Gamma_M^7 + (3.5629 \times 10^{10}) \Gamma_M^8 - (6.9687 \times 10^9) \Gamma_M^9]$$

$E_2 = 205.3$ Gpsi for steel material. The actual magnitude for steel was 206 Gpsi, that means the accuracy of Eq. 20 was 99.6%.

In other way, we can get the same result by going direct to Eq. 24.

Now, it was clear that this method depends on comparing between the maximum amplitude (CMA) of the transmission wave before and after passing through the specimen therefore this method was referred CMA while, the most other method depends on time of flying of the wave TFW. Let the modulus of elasticity calculated from CMA and TFW are E_N and E_D , respectively, to do a practical comparing between CMA and one of laws of TFW:

$$E_D = \frac{C_1^2 \rho (1 + \nu) (1 - 2\nu)}{1 - \nu}$$

where, the most of biggest companies in this field like (Olympic company) (OLYMPUS, 2011) depended on this low in its products, to calculate (E_D).

Table 3 explained the percentage of difference ($R_D\%$) and ($R_N\%$) for values of E_D and E_N respectively, relative to E_s where ($R_D = (E_s - E_D)/E_s$), ($R_N = (E_s - E_N)/E_s$), where the other values in this table were took from source Cardarelli (2008) and NDT (2012). In addition, Fig. 10 shows difference in accuracy between CMA and TFW.

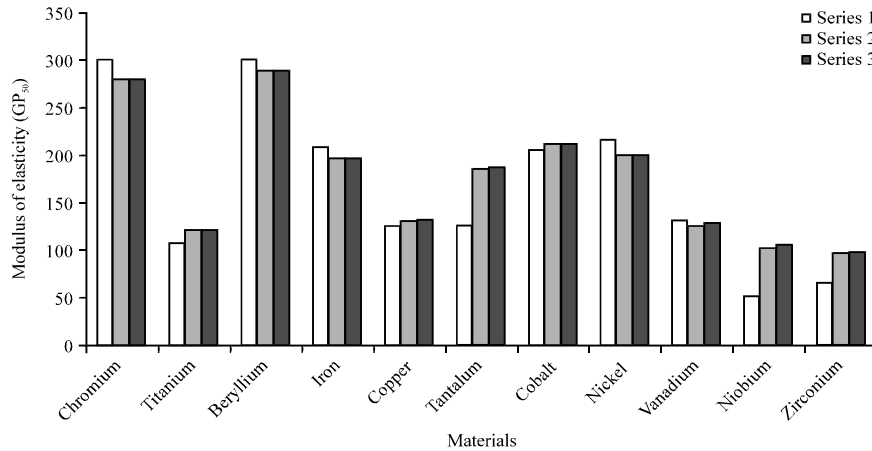


Fig. 10: Comparing between the magnitudes of E_D (blue column) and E_N (green column) relative to magnitude of E_s (red column)

DISCUSSION

The idea of this study depend upon choosing the aluminum as electrodes of the transducer and in the same time as a material to test the other materials. Mason equivalent circuit was chosen to analysis the behavior of PCT, because it take in its account the effect of load in face and back of transducer. During the process of building the transfer function of the transducers, Taylor series for (e^{sT}) in Eq. 15 stopped at term $(sT)^4/4!$ because the Simulink in MATLAB didn't accept less than this value for calculation the response of transfer function of actuator Eq. 19, where $((sT)^4/4! = 4.2424 \times 10^{-27} s)$ is so small comparing with other variables. After the voltage was applied on actuator a stress was directly generated at both aluminum electrodes by piezoelectric coupling, the total force (stress \times area) at each electrode was $h_{33}C_0V$, where each electrode acted as a source of ultrasonic waves, radiating in both positive and negative y-direction as shown in Fig. 2 (Redwood, 1963). Figure 6a and b represented these radiation waves between the two aluminum electrodes as face and back waves for actuator and sensor, respectively, while Fig. 6c and d was zoom out for the front surface wave reflection, where the drawing scale (9.6/85) for time for one wave (distance between two peak of two successive waves) time = 1.1294×10^{-6} sec:

$$\omega = \frac{1}{\text{Time}} = 885 \text{ kHz}$$

This value of frequency identities with the value of frequency in Table 1. The relationships between the output voltage and the modulus of elasticity in

Eq. 24-26 represented final result of this study. CMA test have two advantages than other methods of these field like TFW. First, CMA is more accuracy than TFW, where Fig. 10 illustrated the difference in accuracy between these two methods to calculate the modulus of elasticity relative to real magnitude (E_s). Figure 10 proved the difference between E_D and E_s is irregular, as example E_D is more than E_s for beryllium and iron while for cobalt and copper is less. Table 3 in appendix (a) give us a more details about TFW and CMA, where this table proved TFW is un successful for testing refractory metals (these materials are usually classified as metals having a high melting point), where R_D for these materials such as Tantalum, Zirconium and Niobium equal (33.1, 34.9 and 52.3%). This increase in the amount of R_D is probably due to chemical structure and atomic for these metals, while R_N for these materials did not succeed 2.4%. In spite of the difference between E_s (16 Gpa) and E_N (16.935 Gpa) for lead is not so far but R_N for it is the biggest value (5.8%) in this table for CMA, because $\rho \times E$ for lead is less than $\rho \times E$ of aluminum, where the Eq. 20-22 is applied for materials that have $\rho \times E$ more than $\rho \times E$ for the aluminum. This test need to know the acoustic impedance of the material before doing the test, where this CMA is not suitable for the materials have acoustic impedance lower than the acoustic impedance of aluminum, this may be regarded as the disadvantage of this technique.

The second advantage of CMA is that it is less costly than TFW, where TFW uses two types of PCT first one for generating longitudinal wave and the other type is for generating shear wave (C_s) for calculation Poisson's ratio ν :

Table 3: Properties of different materials and difference percentage between E_D and E_N relative to E_s

Common and trade name	Density ρ (kg m ⁻³)	Longitudinal velocity C_L (m sec ⁻¹)	Poisson's ratio (ν)	Static modules E_s (GPa)	Dynamic modules E_D (GPa)	Difference percentage R_D %	New modules E_N (GPa)	Difference percentage R_N %
Tantalum	16654	3400	0.342	185.7	124.08	33.10	185.40	0.20
Zirconium	6506	4262	0.38	97.0	63.13	34.90	95.10	1.90
Niobium	8570	3480	0.397	104.0	49.53	52.30	101.50	2.40
Chromium	7190	6850	0.21	279.0	299.71	7.42	279.10	0.03
Titanium	4450	6100	0.345	120.0	105.41	12.15	120.01	0.008
Beryllium	1850	12800	0.075	287.0	299.42	4.32	287.00	0.00
Iron	7800	5900	0.29	196.0	207.20	5.71	195.40	0.30
Rhodium	12410	6190	0.26	379.0	388.63	2.54	378.30	0.50
Tungsten	19300	5180	0.28	411.0	405.09	1.40	410.89	0.04
Copper	8941	4660	0.343	130.0	124.62	4.13	129.30	0.53
Steel 4340	7800	5850	0.28	206.0	208.80	1.35	205.30	0.30
Silver	10500	3640	0.367	82.7	79.92	3.37	80.50	2.60
Aluminum	2699	6350	0.35	70.0	67.81	3.12	70.00	0.00
Tin	7298	3320	0.36	50.0	47.86	4.28	49.98	0.04
Lead	11350	2050	0.44	16.0	14.72	8.00	16.935	5.80
Zinc	7133	4170	0.249	104.0	103.55	0.004	101.30	2.50
Cobalt	8900	5730	0.32	211.0	204.21	3.210	210.85	0.07
Nickel	8902	5810	0.312	199.5	215.46	8.02	199.66	0.082
Ruthenium	12370	6530	0.25	432.0	439.56	1.75	432.40	0.09
Rhodium	12410	6190	0.26	379.0	388.63	2.54	378.39	0.16
Molybdenum	10220	6370	0.293	325.0	313.52	3.53	325.10	0.03

$$\nu = \frac{1 - 2(C_s / C_L)^2}{2 - 2(C_s / C_L)}$$

while CMA just need one type of piezoelectric (thickness mode) to generate longitudinal wave.

CONCLUSION

The result of this study proved matters for TFW test. First, the difference between real value of E_s and E_D is irregular. Second, this test is unsuccessful for testing refractory metals, where the difference between E_s and E_D is very large. The new approach CMA was investigated in this study to find the modulus of elasticity for a large range of materials. After building the mathematical model for two PCT ultrasonic transducers (actuator and sensor), we can say the Mason equivalent circuit (Transmission line technique) is one of the best method to analyzing and representing piezoelectric transducer that have two electrodes. On the other hand, the results proved that the relationship for the wave transmission efficiency, resulting from changing in the metals (between the aluminum and the other metals), was smooth and decreases gradually with increasing the magnitude of (density×modulus of elasticity $\rho_2 \times E_2$) for other metals. In addition, the new polynomial equation with excellent identity for this relationship was driven. Finally, according to the considerations of this study, a nice relationship between the output voltage from this system and the modulus of elasticity for a widely range of the metals was driven and obtain too.

REFERENCES

Alwi, H.A.B., J.R. Carey and B.V. Smith, 1996. Chirp response of a single-plate transducer. *J. Acoust. Soc. Am.*, 100: 3655-3664.

Alwi, H.A.B., J.R. Carey and B.V. Smith, 2000. Chirp response of an active-controlled thickness-drive tunable transducer. *J. Acoust. Soc. Am.*, 107: 1363-1373.

Bastida, S., J.I. Eguiazabal, M. Gaztelumendi and J. Nazabal, 1998. On the thickness dependence of the modulus of elasticity of polymers. *Polym. Test.*, 17: 139-145.

Bray, S.L., J.W. Ekin and R. Sesselmann, 1997. Tensile measurements of the modulus of elasticity of Nb/sub 3/Sn at room temperature and 4 K. *IEEE Trans. Applied Supercond.*, 7: 1451-1454.

Builes, M., E. Garcia and C.A. Riveros, 2008. Dynamic and static measurements of small strain moduli of toyoura sand. *Revista Facultad De Ingenieria Universidad De Antioquia*, 43: 86-101.

Cardarelli, F., 2008. *Materials Handbook: A Concise Desktop Reference*. 2nd Edn., Springer, New York, Pages: 1340.

Challis, R.E. and J.A. Harrison, 1983. Rapid solutions to the transient response of piezoelectric elements by z-transform techniques. *J. Acoust. Soc.*, 74: 1673-1680.

Chao, M.C., T.Y. Wu, Z. Wang and C.L. Wang, 2001. Electromechanical coupling factor k_{35}^2 of thickness-shear mode of the piezoelectric thin films deposited on substrates. *Proceedings of the IEEE ULTRASONICS Symposium*, October 7-10, 2001, Atlanta, GA., USA., pp: 464-466.

- Chen, F.M., G.X. Zhao, L.S. Zhang, J.Y. Guo, H.X. Yang and Z.M. Li, 2009. Investigation of resistivity's abnormality and Moduli of elasticity softening in NiTi shape memory alloy. Proceedings of the IEEE 3rd International Conference on Bioinformatics and Biomedical Engineering, June 11-13, 2009, Beijing, pp: 1-4.
- Chow, K.P. and G.A. Millos, 1999. Measurements of modulus of elasticity and thermal contraction of epoxy impregnated niobium-tin and niobium-titanium composites. IEEE Trans. Applied Supercond., 9: 213-215.
- Ciccotti, M. and F. Mulargia, 2004. Differences between static and dynamic elastic moduli of a typical seismogenic rock. Geophys. J. Int., 157: 474-477.
- Dehghan, S., G.H. Sattari, S.C. Chelgani and M.A. Aliabadi, 2010. Prediction of uniaxial compressive strength and modulus of elasticity for Travertine samples using regression and artificial neural networks. Mining Sci. Technol. (China), 20: 41-46.
- Diaz, C.A., K.A. Afrifah, S. Jin and L.M. Matuana, 2011. Estimation of modulus of elasticity of plastics and wood plastic composites using a Taber stiffness tester. Compos. Sci. Technol., 71: 67-70.
- Eurocode1, 2003. Basis of design and actions on structures: Part 4 actions in silos and tanks. European Committee for Standardization, 36: B-1050 Brussels.
- Fabijanski, P. and R. Lagoda, 2008. Genetic identification of parameters the sandwich piezoelectric ceramic transducers for ultrasonic systems. Proceedings of the 13th Power Electronics and Motion Control Conference, September 1-3, 2008, Poznan, pp: 2055-2058.
- Fabijanski, P. and R. Lagoda, 2010. Genetic Identification of Parameters the Piezoelectric Transducers for Digital Model of Power Converter in Ultrasonic Systems. In: Piezoelectric Ceramics, Suaste-Gomez, E. (Ed.). Sciyop Publisher, Croatia, pp: 129-144.
- Fang, J., P. Joos, K. Lunkenheimer and M. van Uffelen, 1995. Study of the modulus of elasticity by linear compression of an adsorbed layer. Colloids Surf. A: Physicochem. Eng. Aspects, 97: 271-278.
- Forster, F. and P.W. Koster, 1939. Modulus of elasticity and damping in relation to the state of the material. J. Inst. Electr. Eng., 84: 558-580.
- Garnier, V. and G. Corneloup, 1996. Determining the evolution of the elasticity modulus by surface waves according to the depth in a nitrated layer. Ultrasonics, 34: 401-404.
- Gokceoglu, C. and K. Zorlu, 2004. A fuzzy model to predict the uniaxial compressive strength and the modulus of elasticity of a problematic rock. Eng. Applic. Artif. Intell., 17: 61-72.
- Gominski, J.P., D.C. dalMolin and C.S. Kazmierczak, 2004. Study of the modulus of elasticity of polymer concrete compounds and comparative assessment of polymer concrete and portland cement concrete. Cem. Concr. Res., 34: 2091-2095.
- Greve, D.W., I.J. Oppenheim and P. Zheng, 2008. Lamb waves and nearly-longitudinal waves in thick plates. Proceedings of the SPIE Conference on Sensors and Smart Structures Technologies for Civil, Mechanical and Aerospace Systems, Volume 6932, March 10-13, 2008, San Diego, CA., USA., pp: 1-10.
- Joseph, E.S. and R.M. Charles, 1996. Stander of Machine Design. McGraw-Hill, New York.
- Krautkramer, J. and H. Krautkramer, 1990. Ultrasonic Testing of Materials. Springer, New York.
- Lee, P.C. and R. Huang, 2002. Mechanical effects of electrodes on the vibrations of quartz crystal plates. IEEE Trans. Ultrasonics Ferroelectrics Frequency Control, 49: 612-625.
- MURATA, 2005. Piezoelectric ceramic sensors (PIEZOTITE®). <http://www.symmetron.ru/suppliers/murata/sensors/p19e6.pdf>
- Mohammed, A.A., S.M. Haris and M.Z. Nuawi, 2014. Influence of a silver epoxy dopant on the performance of broken piezoelectric ceramic transducer based on an analytical model. Smart Mater. Struct., Vol. 23. 10.1088/0964-1726/23/4/045036
- NDT, 2012. Material property tables. <http://www.ndt-ed.org/GeneralResources/MaterialProperties/materialproperties.htm>
- OLYMPUS, 2011. Elastic modulus measurement. <http://www.olympus-ims.com/en/applications/elastic-modulus-measurement/>
- Olympus, 2006. Ultrasonic transducers technical notes. <https://www.olympus-ims.com/data/File/panametrics/UT-technotes.en.pdf>.
- Osamura, K., A. Nyilas and H. Shin, 2010. Estimation of uncertainty with the modulus of elasticity measured by means of tensile test for BSCCO tapes. Cryogenics, 50: 660-665.
- Piazza, G., R. Abdolvand, G.K. Ho and F. Ayazi, 2004. Voltage-tunable piezoelectrically-transduced single-crystal silicon micromechanical resonators. Sensors Actuators A: Phys., 111: 71-78.
- Redwood, M., 1963. A Study of Waveforms in the Generation and Detection of Short Ultrasonic Pulses. Defense Technical Information Center, Belvoir, VA.

- Sofla, M.S., S.M. Rezaei, M. Zareinejad and M. Saadat, 2010. Hysteresis-observer based robust tracking control of piezoelectric actuators. Proceedings of the American Control Conference, June 30-July 2, 2010, Baltimore, MD., pp: 4187-4192.
- Stasiak, M., M. Molenda and J. Horabik, 2007. Determination of modulus of elasticity of cereals and rapeseeds using acoustic method. *J. Food Eng.*, 82: 51-57.
- Vendra, L. and A. Rabiei, 2010. Evaluation of modulus of elasticity of composite metal foams by experimental and numerical techniques. *Mater. Sci. Eng.: A*, 527: 1784-1790.